A Robust Multiphase Power Flow for General Distribution Networks

Murat Dilek, Francisco de León, *Senior Member, IEEE*, Robert Broadwater, *Member, IEEE*, and Serena Lee, *Member, IEEE*

***Abstract*—This paper presents a sweep-based three-phase power flow method for solving general distribution networks that can be heavily meshed and include transformers around the meshes/loops. A load-stepping technique is proposed for solving common convergence problems of sweep-based load-flow solvers when dealing with overloaded radial sections. The proposed power-flow algorithm is based on the iterative solution of radial subsystems assembled together with the mesh equations to comply with Kirchhoff equations. The proposed method is robust and efficient for the solution of heavily loaded systems. Examples are presented for illustration.**

***Index Terms*—Distribution networks, iterative solutions, load flow, sweep-based methods.**

I. Introduction

POWER flow in transmission and distribution networks is computed with different methodologies. The reason is that transmission networks present different characteristics than distribution networks and the algorithms developed for one type of system do not work efficiently on the other.

On one hand, transmission systems are typically three-phase, highly meshed and mostly operate balanced. Current algorithms for the analysis of transmission systems rely on the positive sequence representation of the three-phase system. The most common computational methodology is still the fast decoupled power flow method proposed by Stott and Alsaç in 1974 [1]. Often, however, this method fails to converge when the power system is close to its operating limits and when the R/X ratios of the transmission lines are high. A first alternative is the use of the (full) Newton–Raphson power flow as described by Tinney and Hart in 1967 [2]. Although it has excellent convergence properties, even under stressed circumstances, the Jacobian matrix needs to be factorized at every iteration. Additionally, convergence is only assured when the initial point is sufficiently close to the solution.

On the other hand, distribution systems can have any number of phases, are generally lightly meshed, and unbalanced. In recent years, a current injection method (TCIM) has been proposed [3], [4] for large-scale distribution system analysis, applying the Newton method and modern sparse techniques. Most distribution systems are radial. Forward/backward sweep [5] (FBS) methods take advantage of the radial nature and have become the preferred method by many distribution system analysis programs. Building on the sweep-based approach, [6] and [7] proposed a method for the analysis of lightly meshed systems. With the method, the system is broken into radial subnetworks by opening loops at break points to form a tree. The resulting radial subnetworks are solved efficiently with forward and backward sweeps. A break-point impedance matrix is constructed by a multiport compensation technique and used to solve the integrated system mesh equations. The methodology is based on current injections applied at break-point nodes and lacks in efficiency as the system becomes heavily meshed.

An improvement over [6] was developed in [8]. The method in [8] uses the network graph to construct the sensitivity matrix (equivalent to the break-point impedance matrix in [6]), and thus saves significant execution time by avoiding costly compensation procedures. Also, it uses power flows (P, Q), instead of currents, for break-point injections so that *PV* buses can be handled in a more direct manner.

The load flow methodology described in this paper relies on the same basic approach as [6] and [8]. That is, 1) forward/backward sweeps are applied to solve the system after the system is made radial at the break points, and 2) current-flow injection determined by using a sensitivity matrix is performed at break points.

All calculations are performed in units of volts, amps, and ohms. Per unit calculations are not employed. The modeling encompasses multiphase systems containing three-phase, two-phase, and one-phase components with impedance imbalances, load imbalances, and transformers with legs of different sizes. With this modeling approach impedances must be reflected accordingly when transformers are involved in the sensitivity matrix formulation.

The following important methodology improvements are introduced in this paper: 1) A load-stepping technique that is insensitive to break-point locations allows for the solution of very heavily loaded systems. 2) Loops that need special handling when transformers are involved can be analyzed. 3) The approach of this paper does not need to set the voltages of break points close to their nominal values (magnitude and angle). 4) The algorithm has been efficiently implemented with *iterators* [9], [11], [12], [14]. 5) The sensitivity matrix is obtained very efficiently by simply adding the impedance of the elements around the loop with the feeder-path traces [12]. These improvements

Manuscript received January 13, 2009; revised June 10, 2009. First published December 31, 2009; current version published April 21, 2010. Paper no. TPWRS-00990-2008.

M. Dilek is with Electrical Distribution Design, Inc., Blacksburg VA 24060 USA.

F. de León is with the Polytechnic Institute of NYU, Brooklyn, NY 11201 USA (e-mail: fdeleon@poly.edu).

R. Broadwater is with Virginia Tech, Blacksburg VA 24060 USA.

S. Lee is with Consolidated Edison of New York, New York, NY 10003 USA (e-mail: leese@coned.com).

Color versions of one or more of the figures in this paper are available online at http://ieeexplore.ieee.org.

Digital Object Identifier 10.1109/TPWRS.2009.2036791

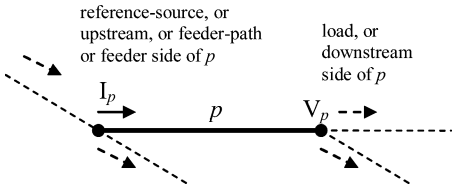

Fig. 1. Convention for the current and voltage of a component.

make possible the effective analysis of large heavily meshed secondary networks with FBS.

II. Review of Radial Power Flow

The radial power flow algorithm relies on forward and backward sweeps that are repeated until a convergence criterion is met. In our study forward and backward sweeps are named as "forward trace" and "reverse trace", respectively [9], [10]. For a component p in a circuit (Fig. 1), the current of p, I_p, is represented by the current flowing into p at its feeder-path end, whereas the voltage of p is represented by the voltage occurring at its other end where the current leaves the component. Component p might have shunt currents, too. In such a case, the component current I_p is the sum of the shunt currents and the current leaving p. For transformer components the leaving currents are accordingly reflected to the feeder-path side. With loads present, I_p will involve both the load currents and the currents leaving the component towards the downstream components. Loads may be distributed over a line or a cable.

The voltage of the root node or the reference source is always known. Currents are first initialized to zero. Then, iterations start in order to find converging voltage and current values. At a given radial power flow iteration, voltages are calculated by performing the forward trace in which existing currents are used. Then, the reverse trace is carried out to recalculate/update the existing currents by using the newly calculated voltages from the forward trace. These forward and reverse trace calculations are continued until convergence occurs or the algorithm runs a specified number of iterations.

Topology iterators such as the forward iterator and the backward iterator are used for tracing through the components [11], [12].

1) Convergence Criterion: The convergence is decided by checking the percent change in current that occurs at the root node between the previous and the current iteration. As an example, a 0.05% convergence criterion for change in current works well for many distribution systems. With this convergence criterion, the algorithm will stop at some iteration k if

$$100 \times \frac{\left|\mathrm{I}_r^{(k)} - \mathrm{I}_r^{(k-1)}\right|}{\left|\mathrm{I}_r^{(k-1)}\right|} \leq 0.05$$

where $\mathrm{I}_r^{(k)}$ and $\mathrm{I}_r^{(k-1)}$ are the currents (with magnitude and angle) of the reference source as calculated at iterations k and $k-1$, respectively. Note that for a three-phase reference source I_r will have three currents, and the convergence criterion is met individually for each phase.

2) Forward Trace: The calculation starts at the source (or root node) where the voltage is known. Voltages are then calculated at the downstream components, following the order given by the forward iterator. The forward iterator ensures that when the calculation comes to voltage evaluation at a component p, the voltage for the feeder-path of p has already been calculated. The voltage across p is calculated according to the characteristics pertinent to p. Therefore, each component can embed its own across (voltage drop) calculation during the forward trace.

3) Reverse Trace: All currents are first reset to zero. The reverse trace uses the voltages from the forward trace. The calculation starts at end components and moves toward the source, following the order given by the backward iterator. The backward iterator ensures that when the calculation arrives at the calculation of current at component p, currents at all downstream components have already been evaluated. Because of this processing order, the current of p, I_p, has already been set to some value corresponding to the current feeding all downstream components. In the reverse trace at p, I_p is updated with the additional currents that come from inside p, such as internal loads or admittances. Because I_p is assumed to come from the feeder path of p, the current at the feeder component of p is then updated by adding I_p to it.

The radial power flow algorithm is summarized as follows.

1) Initialize: Set all currents to zero. Set counter $k = 1$.
2) Calculate voltages by the forward trace.
3) Calculate currents by the reverse trace.
4) Check convergence: If $k > 1$ and the convergence criterion is met, stop; else, go to Step 5.
5) Update counter, $k = k + 1$. If $k > k_{\max}$, stop (no converging solution found); else, go to Step 2.

III. Network Power Flow Analysis

The network power flow analysis builds on the radial system analysis. As part of the network analysis the system is "radialized". The radialization is performed by breaking the existing independent loops at certain points referred to as "cotrees" [13]. The radial power flow is run on the radialized network. The radial solutions result in voltage disagreements across the broken cotree points. Using current injections and extractions, a correction process is employed until the voltages across the cotrees closely agree. The radial power flow and the correction process are repeated until all cotree voltage gaps fall below negligibly small values

The correction process basically consists of injecting current at one side of the cotree while extracting the same amount of current out of the other side of the cotree. The injection/extraction currents are determined using a sensitivity matrix. The sensitivity matrix represents the relationship between the cotree voltage gaps and currents that can be injected/extracted at cotree points. Therefore, the way the sensitivity matrix is formulated plays a central role in the success of the network power flow calculation.

A. Sensitivity Matrix Formulation For Single-Loop Networks

The procedure for sensitivity matrix formulation is now explained using the single-loop network shown in Fig. 2. The net-

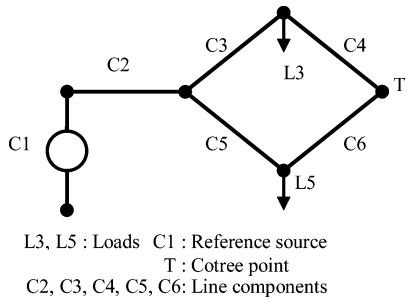

Fig. 2. Simple network with one loop.

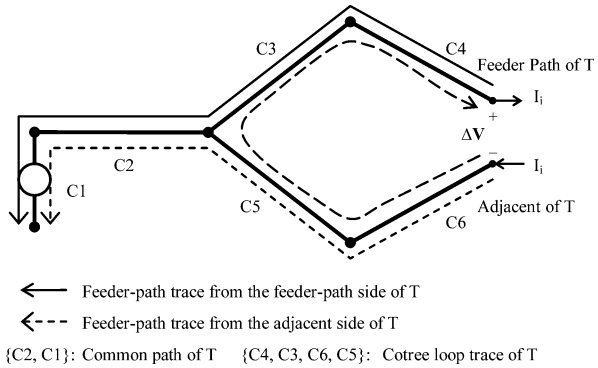

Fig. 3. Network of Fig. 2 as radialized for power flow analysis.

work has one reference source C1. The common point T between C4 and C6 is the cotree point where the system is to be radialized for analysis (Fig. 3). Assume the power flow is performed on the radialized system, resulting in a voltage difference $\Delta\mathbf{V}$ across T. For a three-phase system, $\Delta\mathbf{V}$ involves three voltage differences.

Each cotree involves an adjacent component and a feeder path component [10]–[13]. The cotree voltage gap is defined as the voltage difference between the feeder-path side and the adjacent side of the cotree point. In this case C4 and C6 become the feeder-path and adjacent sides of T, respectively. Ignoring the effects of loads and any other shunt elements, the voltage gap is expected to disappear if the current injection/extraction is selected properly, illustrated in Fig. 3 with $\mathrm{I_i}$. The injected current is determined by

$$\mathbf{S}\mathbf{I}_\mathrm{i} = \Delta\mathbf{V} \tag{1}$$

where $\mathbf{S} = \mathbf{Z}_4 + \mathbf{Z}_3 + \mathbf{Z}_5 + \mathbf{Z}_6$; and $\mathbf{Z}_4$, $\mathbf{Z}_3$, $\mathbf{Z}_5$, and $\mathbf{Z}_6$ are the impedances of C4, C3, C5 and C6, respectively. $\mathbf{S}$ in (1) is referred to as the sensitivity matrix. Here $\mathbf{I}_\mathrm{i}$ represents three phase currents while $\Delta\mathbf{V}$ corresponds to three phase voltage gaps. Hence, $\mathbf{S}$ is a 3×3 matrix. $\mathbf{S}$ is formulated as follows.

1) Reset $\mathbf{S} = 0$.
2) Find the first common-path component $(\mathrm{C_{cp}})$ associated with T.
   2a) Start from the feeder-path side of T, mark components as moving along the feeder path until the reference source. In Fig. 3, components $\{\mathrm{C4},\ \mathrm{C3},\ \mathrm{C2},\ \mathrm{C1}\}$ will be marked by this trace.
   2b) Start from the adjacent side of T, move along the feeder path, stop if a component marked by (2a) is encountered, identifying this component as $\mathrm{C_{cp}}$. In Fig. 3 C2 will be identified as $\mathrm{C_{cp}}$.
3) Start from the feeder-path side of T, add impedances to $\mathbf{S}$ as moving along the feeder path until $\mathrm{C_{cp}}$ is encountered. Do not include $\mathrm{C_{cp}}$. In Fig. 3 this trace will include $\{\mathrm{C4},\ \mathrm{C3}\}$.
4) Start from the adjacent side of T, add impedances to $\mathbf{S}$ as moving along the feeder path until $\mathrm{C_{cp}}$ is encountered. Do not include $\mathrm{C_{cp}}$. In Fig. 3 this trace will include $\{\mathrm{C6},\ \mathrm{C5}\}$.

The common-path of a cotree consists of those components that are encountered in both feeder-path traces which are performed from the feeder-path and adjacent sides of the cotree. In Fig. 3 components $\{\mathrm{C2},\ \mathrm{C1}\}$ form the common-path for T. Also, the union of the components that are encountered in steps 3–4 above constitutes the loop trace for the cotree.

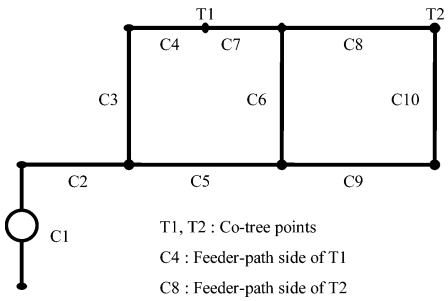

Fig. 4. Simple example for multiloop network.

B. Sensitivity Matrix for Multiloop Networks

The procedure to obtain the sensitivity matrix consists of adding component impedances to the sensitivity matrix as moving along cotree loop traces. When a component is visited on a cotree loop trace, it is checked if the same component is included in other cotree loop traces. If so, the impedance of the component is added to $\mathbf{S}$ at the matrix entry corresponding to the cotrees involved.

The component impedance is added to $\mathbf{S}$ according to the type of cotree paths. The impedance is added if two cotrees have the component on the same type of path. That is, the component is either on the feeder-path side of both cotrees, or on the adjacent-side feeder path of both cotrees. On the other hand, the negative of the impedance is added if the two cotrees have the component on different path types (i.e., one is a feeder path trace and the other is an adjacent feeder path trace).

Consider the network shown in Fig. 4. This three-phase network has two loops associated with the cotree points T1 and T2. The sensitivity matrix $\mathbf{S}$ is a 2×2 block matrix, where each block is given as a 3×3 matrix. $\mathbf{S}_{12}$, for instance, will correspond to a 3×3 matrix representing the mutual coupling between T1 and T2.

Cotree paths and traces are detailed in Fig. 5. Note that C6 is the only component that is included in the loop traces of both cotrees. Also C6 is on the adjacent feeder path trace of T1 and the feeder trace of T2. Therefore, the mutual terms $\mathbf{S}_{12}$ and $\mathbf{S}_{21}$ will involve the negative of the component impedance $(-\mathbf{Z}_6)$. $\mathbf{S}$ is formulated as follows.

1) Reset $\mathbf{S} = 0$, and set the cotree index $\mathrm{i} = 1$.

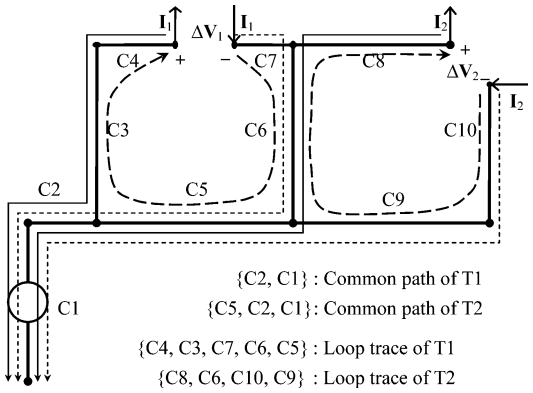

Fig. 5. Network of Fig. 4 as radialized at cotree points for current injection.

2) Starting from the feeder path side of $\mathrm{T_i}$, trace the feeder path. For each component $\mathrm{C_k}$ on the path do the following:
   2a) If $\mathrm{C_k}$ is the first common path component of $\mathrm{T_i}$, stop the trace and go to Step 3.
   2b) Add $\mathbf{Z}_{\mathrm{k}}$ to $\mathbf{S}_{\mathrm{ii}}$.
   2c) Check for other cotrees whose cotree loop traces include $\mathrm{C_k}$. For each such cotree $\mathrm{T_j}$, do the following: If $\mathrm{C_k}$ is on the feeder path of $\mathrm{T_j}$, then $\mathbf{S}_{\mathrm{ij}} = \mathbf{S}_{\mathrm{ij}} + \mathbf{Z}_{\mathrm{k}}$; else, $\mathbf{S}_{\mathrm{ij}} = \mathbf{S}_{\mathrm{ij}} - \mathbf{Z}_{\mathrm{k}}$.
3) Starting from the adjacent side of $\mathrm{T_i}$, trace the feeder path. For each component $\mathrm{C_k}$ on the path, do the following:
   3a) If $\mathrm{C_k}$ is the first common path component of $\mathrm{T_i}$, stop the trace and go to Step 4.
   3b) Add $\mathbf{Z}_{\mathrm{k}}$ to $\mathbf{S}_{\mathrm{ii}}$.
   3c) Check for other cotrees whose cotree loop traces include $\mathrm{C_k}$. For each such cotree $\mathrm{T_j}$ found, do the following:
   If $\mathrm{C_k}$ is on the adjacent-side feeder path of $\mathrm{T_j}$, then $\mathbf{S}_{\mathrm{ij}} = \mathbf{S}_{\mathrm{ij}} + \mathbf{Z}_{\mathrm{k}}$; else, $\mathbf{S}_{\mathrm{ij}} = \mathbf{S}_{\mathrm{ij}} - \mathbf{Z}_{\mathrm{k}}$.
4) Consider the next cotree: $\mathrm{i} = \mathrm{i} + 1$, if $\mathrm{i} > \mathrm{i}_{\max}$ stop; else, go to Step 2.

According to the procedure above, the network of Fig. 4 has the sensitivity matrix shown in the equation at the bottom of the page. Cotree injection currents are determined by solving

$$\begin{bmatrix} \mathbf{S}_{11} & \mathbf{S}_{12} \\ \mathbf{S}_{21} & \mathbf{S}_{22} \end{bmatrix} \begin{bmatrix} \mathbf{I}_1 \\ \mathbf{I}_2 \end{bmatrix} = \begin{bmatrix} \Delta\mathbf{V}_1 \\ \Delta\mathbf{V}_2 \end{bmatrix}.$$

C. Sensitivity Matrix for Loops With Transformers

Transformers are modeled such that transformer impedances are assumed to be reflected to the load side. Consider Fig. 6. The transformer current and voltage are represented by $\mathbf{I}_p$ and $\mathbf{V}_p$ as shown. $\mathbf{V}_{p'}$ represents the internal voltage where the feeder-side voltage ($\mathbf{V}_{pfd}$) is ideally transformed. The load-side voltage is obtained after subtracting from this internal voltage the voltage

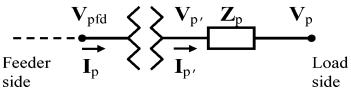

Fig. 6. Model for a transformer component p.

drop due to transformer impedance. To simplify the discussion, transformer magnetizing currents are neglected.

For the sensitivity matrix formulation, two matrices (denoted by $\mathbf{K}_{\mathrm{V}}$ and $\mathbf{K}_{\mathrm{I}}$) are defined in order to perform the following transformations:

$$\mathbf{V}_{p'} = \mathbf{K}_{\mathrm{V}}\mathbf{V}_{pfd}$$
$$\mathbf{I}_p = \mathbf{K}_{\mathrm{I}}\mathbf{I}_{p'}$$

where

$\mathbf{K}_{\mathrm{V}}$ voltage-reflection matrix: a 3×3 transformation matrix that reflects the feeder-side voltage to the load side;

$\mathbf{K}_{\mathrm{I}}$ current-reflection matrix: a 3×3 transformation matrix that reflects the load-side current to the feeder side.

A 3×3 complex matrix is used for both reflection matrices. Note that the diagonal entries in the matrices $\mathbf{K}_{\mathrm{V}}$ and $\mathbf{K}_{\mathrm{I}}$ are not necessarily equal. By using the complex matrix, any phase-shift effect with transformer winding connections is incorporated into the reflection process. The effect of off-nominal individual tap positions at each phase can also be included.

The reflection matrices of the transformer are used in case the transformer is encountered in a cotree loop trace during the sensitivity matrix formulation. Note that during loop traces (as performed by Steps 2 and 3 in the previous section) the load side of the transformer becomes the cotree side. The objective is to obtain the source-side voltage as it would appear at the cotree side so that the resulting cotree side voltage can be expressed in terms of the cotree current.

Consider the single-loop network in Fig. 7. The transformer components C3 and C6 are found on the loop trace of cotree point T. Nominally, the loop will have two voltage levels. The sensitivity matrix for this case is shown in the figure. Only component C5 is reflected. The other loop components are already on the cotree-side of the loop.

The general sensitivity-matrix formulation for multiple loops with transformer components will be summarized below. The procedure can be used for networks with general loops where more than one transformer can exist along the path when moving from either of the cotree sides to the cotree common path—that is, loops with two or more voltage levels.

An example is provided in Fig. 8. The network in the figure has two cotrees, T1 and T2. Also, there are two reference

$$\mathbf{S} = \begin{bmatrix} \mathbf{Z}_4 + \mathbf{Z}_3 + \mathbf{Z}_7 + \mathbf{Z}_6 + \mathbf{Z}_5 & -\mathbf{Z}_6 \\ -\mathbf{Z}_6 & \mathbf{Z}_8 + \mathbf{Z}_6 + \mathbf{Z}_{10} + \mathbf{Z}_9 \end{bmatrix}$$

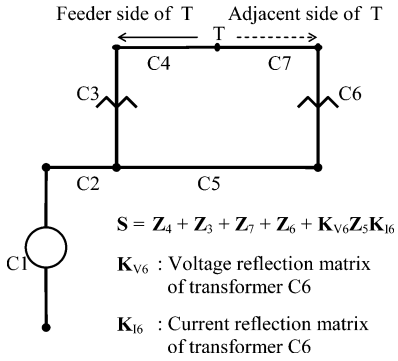

Fig. 7. Sensitivity matrix for a single loop with two transformers (C3 and C6).

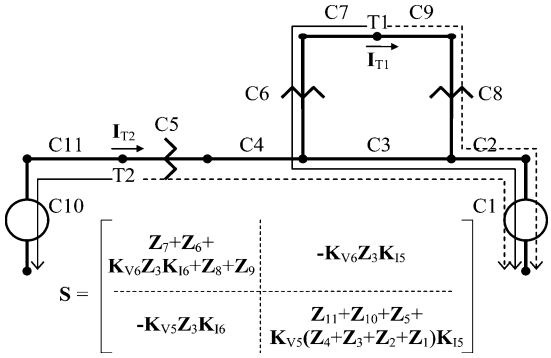

Fig. 8. Sensitivity matrix for a network with two loops and two reference sources.

sources (C1 and C10) such that only C11 is associated with source C10 while the other components are associated with source C1. Feeder path (solid lines) and adjacent traces (dashed lines) are also indicated in the figure. Note that T2, which is associated with different reference sources on its feeder path and adjacent sides, does not have a common path.

C3 is the only mutual component between the cotree traces of T1 and T2. The effect of T2 cotree current on T1 cotree voltage will be $-\mathbf{K}_{V6}\mathbf{Z}_3\mathbf{K}_{I5}\mathbf{I}_{T2}$. Note that the $(-)$ sign is due to C3 having different types of traces from the cotrees. Similarly, T1 cotree current will impact the T2 cotree voltage by $-\mathbf{K}_{V5}\mathbf{Z}_3\mathbf{K}_{I6}\mathbf{I}_{T1}$.

Let $\mathbf{I}$ be 3×3 identity matrix. The steps for sensitivity-matrix formulation procedure are as follows.

1) Reset $\mathbf{S} = 0$, set the cotree index $\mathrm{i} = 1$.
2) Reset $\mathbf{K}_V = \mathbf{I}$, $\mathbf{K}_I = \mathbf{I}$.
3) Starting from the feeder-path side of Ti, trace the feeder path. For each component Ck on the path, do the following:
   3a) If Ck is the first common-path component of $\mathrm{T_i}$, stop the trace and go to Step 4.
   3b) Add $\mathbf{K}_V\mathbf{Z}_k\mathbf{K}_I$ to $\mathbf{S}_{ii}$.
   3c) Check for other cotrees whose cotree loop traces include Ck. For each such cotree $\mathrm{T_j}$ found, do the following:
   - Reset $\hat{\mathbf{K}}_I = \mathbf{I}$.
   - Perform feeder path trace from $\mathrm{T_j}$ to Ck (not included). At each transformer component Cr, update $\hat{\mathbf{K}}_I = \hat{\mathbf{K}}_I\mathbf{K}_{Ir}$.
   - If Ck is in the feeder path of $\mathrm{T_j}$, then $\mathbf{S}_{ij} = \mathbf{S}_{ij} + \mathbf{K}_V\mathbf{Z}_k\hat{\mathbf{K}}_I$; else, $\mathbf{S}_{ij} = \mathbf{S}_{ij} - \mathbf{K}_V\mathbf{Z}_k\hat{\mathbf{K}}_I$.

   3d) If Ck is a transformer component update:

$$\mathbf{K}_V = \mathbf{K}_{Vk}\mathbf{K}_V,\ \mathbf{K}_I = \mathbf{K}_{Ik}\mathbf{K}_I.$$

4) Reset $\mathbf{K}_V = \mathbf{I}$, $\mathbf{K}_I = \mathbf{I}$.
5) Starting from the adjacent side of Ti, trace the feeder path. For each component Ck on the path, do the following:
   5a) If Ck is the first common path component of Ti, stop the trace and go to Step 4.
   5b) Add $\mathbf{K}_V\mathbf{Z}_k\mathbf{K}_I$ to $\mathbf{S}_{ii}$.
   5c) Check for other cotrees whose cotree loop traces include Ck. For each cotree Tj found, do the following:
   - Reset $\hat{\mathbf{K}}_I = \mathbf{I}$.
   - Perform feeder path trace from Tj to Ck (not included). At each transformer component Cr, update $\hat{\mathbf{K}}_I = \hat{\mathbf{K}}_I\mathbf{K}_{Ir}$.
   - If Ck is on the adjacent-side feeder path of Tj, then $\mathbf{S}_{ij} = \mathbf{S}_{ij} + \mathbf{K}_V\mathbf{Z}_k\hat{\mathbf{K}}_I$; else, $\mathbf{S}_{ij} = \mathbf{S}_{ij} - \mathbf{K}_V\mathbf{Z}_k\hat{\mathbf{K}}_I$.

   5d) If Ck is a transformer component update:

$$\mathbf{K}_V = \mathbf{K}_{Vk}\mathbf{K}_V, \quad \mathbf{K}_I = \mathbf{K}_{Ik}\mathbf{K}_I.$$

6) Consider the next cotree: update $\mathrm{i} = \mathrm{i}+1$, if $\mathrm{i} > \mathrm{i_{max}}$ stop; else, go to Step 2.

D. Network Power Flow Algorithm

In the network power flow analysis the cotree voltage updates using the current injection process are repeated until the convergence criterion is met or until the number of iterations exceeds a specified value. The convergence criterion used is voltage differences across all cotrees are less than a specified percent of nominal cotree voltages. A convergence criterion of 0.02% works well for many distribution networks. With this figure, if a cotree is located at a primary point in a 13.2-kV grounded-wye distribution circuit, the line-to-ground voltage difference across each phase of the cotree is less than 1.52 V. The algorithm steps are summarized as follows.

1) Reset network power flow iteration counter $\mathrm{k} = 0$.
2) Calculate and perform an LU-decomposition of the sensitivity matrix $\mathbf{S}$.
3) Reset cotree injection currents, $\mathbf{I_i} = 0$.
4) Run radial power flows.
5) Check for network convergence. If converged, stop.
6) Find cotree injection currents using $\mathbf{S}\Delta\mathbf{I_i} = \Delta\mathbf{V_i}$, where $\Delta\mathbf{I_i}$ represents the needed change in cotree injection currents.
7) Update the cotree injection currents: $\mathbf{I_i} = \mathbf{I_i} + \Delta\mathbf{I_i}$.
8) Execute the next network iteration: $\mathrm{k} = \mathrm{k}+1$, if $\mathrm{k} > \mathrm{k_{max}}$, stop (no converging solution found); else, go to Step 4.

The sensitivity matrix is calculated once and is not updated for every network iteration unless the network topology changes throughout the analysis. Also, the matrix is LU-decomposed once, and used at every iteration with new $\Delta\mathbf{V_i}$ values.

When the effect of loads and shunt elements are not considered, the voltage gaps are expected to disappear in one iteration, by the injected currents. However, because of the nonlinear loads and the existing shunt elements that are not involved in

the sensitivity matrix calculation, it may in practice take several network iterations before all the voltage gaps come close to negligibly small amounts. Therefore, the number of iterations depends on the number of nonlinear loads and shunt elements as well as the number of loops being solved. In typical distribution networks, convergence is achieved within a few iterations (generally less than five).

As the number of loops grows, Step 2 starts dominating the total execution time of the power flow analysis. In addition to the number of loops, the effect becomes more pronounced with denser (i.e., less sparse) sensitivity matrices. Therefore, the sparsity of the matrix is exploited by avoiding unnecessary complex number multiplications in order to speed the process in Step 2.

IV. Network Power Flow With Load Stepping

The radial power flow is a key computational module of the network power flow. The radial power flow must converge first, in order for the network power flow to proceed with the current-injection process. If the cotree points, where the network is radialized, are not strategically selected, then the radial power flow might fail to converge due to the fact that some sections of the network pick up an unrealistically high load while some other sections become lightly loaded. In other words, due to the placement of cotree points, a radial section might initially carry much more power than it would have in the final converged solution, even to the point of the static stability limits of the lines being exceeded and no radial solution existing. While one could pre-examine the network in order to ensure that the cotrees are located so that the radialized solutions converge, with large networks this would be a tedious task.

Here a technique is used to assure that the radial power flow does not fail due to improper cotree locations. The technique starts the radial power flow with reduced loads (that is, loads are scaled to a very small percentage) instead of using the actual loads. With all loads uniformly scaled-down, it is much easier for the radial power flow to converge, therefore, obtaining an initial network power flow solution (where cotree currents are obtained). Loads are then increased to the next level. By comparing the new loading with the previous one, which has a converging solution, cotree currents are estimated for the new loading level. With the estimated cotree currents in place, the radial power flow will converge easier than with the case where no initial cotree currents exist. The network power flow solution is then obtained at the new loading level, and then the loads are stepped again until the full loading level is achieved. The procedure is summarized below.

1) Set loading-level index $\mathrm{k} = 1$.
2) Calculate and LU-decompose the sensitivity matrix $\mathbf{S}$.
3) Reset cotree injection currents, $\mathbf{I}_{\mathrm{i}} = 0$.
4) Find the network power flow solution at loading level $\mathrm{u_k}$.
5) If the full loading level ($\mathrm{u_k} = 100\%$) is achieved, stop; else, go to Step 6.
6) Step to the next loading level.
   6a) Update the loading-level index: $\mathrm{k} = \mathrm{k} + 1$.
   6b) Estimate cotree currents for the new loading level: $\mathbf{I}_{\mathrm{i}} = (\mathrm{u_k}/\mathrm{u_{k-1}})\mathbf{I}_{\mathrm{i}}$.
7) Go to Step 4.

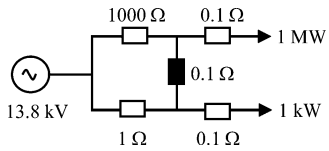

Fig. 9. Meshed network to be broken into radial branches. The break point was selected as the dark $0.1\ \Omega$ branch.

Note that Step 4 above involves the network power flow algorithm steps that are outlined in the previous section, except for Steps 2 and 3, which are now handled in Steps 2 and 3 of this algorithm.

The authors have successfully used two loading steps at $\{0.1\%,\ 100\%\}$ for typical distribution network power flow studies. A first step with a one-thousandth of the load is in most practical cases sufficient to assure convergence of all the radials as it will be shown next. However, the method is completely general and greater load reduction ratios can be implemented in a self-adjusting manner when necessary. Thus, if one or more radial subsystems do not converge after a first load reduction step, a second reduction step could be applied.

For heavily loaded large systems intermediate loading steps may be necessary. Experience with a large number of real systems has shown that loading steps at $\{0.1\%,\ 5\%,\ 100\%\}$ are effective to get the convergence at 100% loading in the third step. The intermediate solution at 5% loading is usually as easy and as fast as that at 0.1%, yet provides much better initial cotree current estimates for 100% loading than does the solution at 0.1% loading.

V. Test Results

A. Convergence Problems With Traditional FBS

When a system is radialized it is possible to create accidentally radial sections that have no solution. Uncharacteristically large loads can be left connected to a weak (high impedance) path. There are two possible solutions to this problem: 1) Implement an algorithm for the (optimal) selection of the location of break points where the current is minimal along the loop (ideally zero); 2) Initialize the current injections to shift the large load current to the strong (small impedance) side of the broken loops. Both require the knowledge of an approximate solution. In this paper we have computed very efficient predictions of the current injections by step loading. Below two examples are presented.

1) Divergent Radial Iterations (Heavy Load): When in the process of selecting the breaking points of a network to obtain a tree (breaking the loops), one or more of the resulting radial subsystems has a (very) heavy load, and the standard solution method diverges. Consider the resistive system depicted in Fig. 9. The best location for the break point is on the $1000\ \Omega$ branch. However, to illustrate the convergence problem and the proposed solution consider that the break point is set on the $0.1\ \Omega$ branch joining the upper and lower sides of the circuit (dark impedance in Fig. 9).

Fig. 10 shows the radial section that cannot be solved with the traditional procedure since it consists of a (very) weak system with a (very) large load. Let us start the conventional iteration

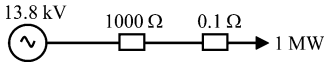

Fig. 10. System with divergent radial iterations due to heavy load because of the non-optimal selection of break points.

procedure with a flat start: $V_{Load}^{(0)} = 13.8$ kV. The first value of the load current is computed as

$$I_{Load}^{(1)} = \frac{P}{V_{Load}^{(0)}} = \frac{1\,000\,000}{13\,800} = 72.464 \text{ A}.$$

The voltage drop in the series impedances are

$$\begin{aligned} V_{1000} &= (1000)(72.464) = 72\,464 \text{ V} \\ V_{0.1} &= (0.1)(72.464) = 7.2464 \text{ V} \\ V_{Total} &= (1000.1)(72.464) = 72\,471 \text{ V}. \end{aligned}$$

Now the voltage at the load is updated as

$$V_{Load}^{(1)} = 13\,800 - 72\,471 = -58\,671 \text{ V}.$$

The load voltage has a larger and negative value at the first iteration. Following the same procedure, we get the subsequent divergent iterations:

$$\begin{aligned} I_{Load}^{(2)} &= -17.044 \text{ A}; \; V_{Load}^{(2)} = 30\,846 \text{ V} \\ I_{Load}^{(4)} &= -53.699 \text{ A}; \; V_{Load}^{(4)} = 67\,504 \text{ V} \\ I_{Load}^{(6)} &= -984.81 \text{ A}; \; V_{Load}^{(6)} = 99\,870 \text{ V}. \end{aligned}$$

The divergent radial iterations are eliminated by step-loading. Consider the case when the load is reduced by a factor of 1000; thus, the first solution yields

$$\begin{aligned} I_{Load}^{(1)} &= \frac{P}{V_{Load}^{(0)}} = \frac{1000}{13\,800} = 0.072464 \text{ A} \\ V_{Total} &= (1000.1)(0.072464) = 72.471 \text{ V} \\ V_{Load}^{(1)} &= 13\,800 - 72.471 = 13\,727.53 \text{ V}. \end{aligned}$$

With the same procedure, we get the following convergent iterations:

$$\begin{aligned} I_{Load}^{(2)} &= 0.072846 \text{ A}; \quad V_{Load}^{(2)} = 13\,727.146 \text{ V} \\ I_{Load}^{(4)} &= 0.072848 \text{ A}; \quad V_{Load}^{(4)} = 13\,727.144 \text{ V}. \end{aligned}$$

Note that very few iterations are needed to obtain convergence of the radial subsystems. This is so because at this step in the solution the system is (very) lightly loaded and therefore its behavior is linear.

Now, we are in a position to compute the current injection coming from the lower side and step the load up. The voltage in the lower (strong) radial is virtually 13.8 kV because it would be loaded with only 1 W (remember that load has been scaled down 1000 times) and the impedances are small. The sensitivity matrix (S) is the sum of the impedances around the loop: $S = 1001.1\ \Omega$. Therefore, the current injection for the circuit with reduced load is computed as

$$I_{red}^{inj} = \frac{\Delta V}{S} = \frac{13\,800 - 13\,727.44}{1001.1} = 0.072776 \text{ A}.$$

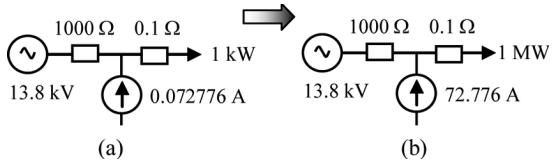

Fig. 11. Procedure to extrapolate the current injection. (a) Reduced load system. (b) Full load system.

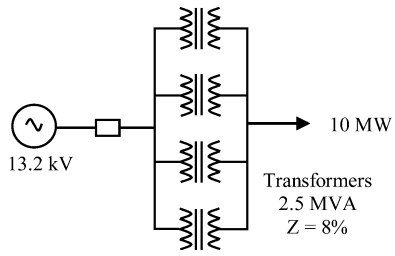

Fig. 12. System with divergent radial iterations due to heavy loading because one transformer will have to carry the entire load at the first iteration.

Fig. 13. System with divergent radial iterations due to a 400% overload.

Fig. 11 illustrates the procedure to extrapolate the current injection from the reduced load system to the full load system. The current injection for the full load is computed by magnifying the current injection of the reduced load by the reduction factor used in load stepping. Note that the injected current (72.776 A) from the adjacent circuit is practically equal to the load current for flat start (72.464 A). This is expected since the load current is mainly supplied from the lower branch and our method is capable to detect this. Additionally, note that none of the circuits in Fig. 11 presents convergence problems; therefore a robust solution has been obtained.

2) Four (or More) Parallel Transformers: A common arrangement in distribution substations is to have four (or more) transformers in parallel supplying a set of feeders; see Fig. 12. Because of the need to break the assembled system into radial subsystems the entire load gets assigned to one of the transformers at the beginning of the simulation as shown in Fig. 13. In our example a load of 10 MW has to be supplied by a 2.5-MVA transformer at the beginning of the simulation. This load is too large for the normal forward-backward sweeps method that fails to converge.

Load stepping as described above has been used successfully for the solution of this kind of systems. Fig. 14 illustrates the intermediate step when the load is reduced 1000 times. This is used to compute the current injections shown in the figure. The solution is obtained very easily in a few iterations since the

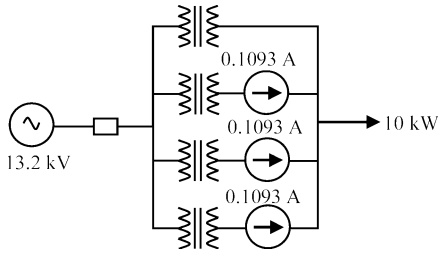

Fig. 14. System with a first estimation of the current injections for a 1000 times reduced load.

TABLE I
DISTRIBUTION TEST SYSTEMS FROM THREE U.S. UTILITIES

System	Size (MVA)	#Load Buses	#Loops	#Lines	#TRs	#Secdry Comps	#Total Comps
Sys1	185	2124	71	14871	2363	5042	29034
Sys2	142	191	113	1260	232	1520	3515
Sys3	14.2	110	92	733	67	958	1249
Sys4	8.7	251	3	698	251	494	1083
Sys5	7	1145	0	2886	1150	2284	4313
Sys6	7.5	51	0	165	51	80	258

system is very lightly loaded. Then the computed current injections (0.1093 A) are magnified 1000 times to give the necessary 109.3 A injection for the solution of the system at full load. This is very close to the actual solution where each transformer supplies 109.7 A to the load operating at 13.157-kV line-to-line.

B. Real Distribution Systems

The approach presented here has been successfully used on a number of very large-scale distribution systems. Six test systems are selected from three U.S. utilities. The test systems are given in Table I, including such system data as size, total numbers of (three-phase) loops, load locations, line and transformer components, as well as secondary and all (primary and secondary) components modeled. The systems model the secondary sides $(\text{voltage} < 480\ \text{V})$ of distribution transformers where most of the loads are placed. The majority of the loops formed are due to network transformers tied at their secondaries. Shunt components are included. The number of secondary components is provided because in our experience large systems with long secondary sections are prone to convergence problems caused by high secondary currents yielding voltage fluctuations in the forward sweep.

Sys1 represents the model of an area of the Staten Island system in New York with 33-kV sub-transmission feeders feeding 4-kV distribution feeders. Most of the loops are formed at the 33-kV level. *Sys2* represents 13-kV primary feeders that supply power into a mid-size secondary network in the metropolitan Manhattan area. Similarly, *Sys3* models a downtown network (fed by 13-kV primary feeders) in St. Louis. *Sys4* and *Sys6* represent two suburban circuits in Detroit, with some commercial and industrial loads. *Sys4* is mostly radial, and the loops are formed at the primary level. *Sys5* models another Detroit circuit that is radial feeding a residential suburban area.

By comparing the number of loops to the number of components it can be said that *Sys1* and *Sys4* are very lightly meshed, while *Sys2* and *Sys3*, are heavily meshed systems corresponding to networked distribution feeders as found in urban cores.

TABLE II
EXECUTION TIMES OF POWER FLOW AS RUN ON TEST SYSTEMS WITH CONSTANT-POWER LOAD MODEL

System	Sens Mx Processing (sec)			Constant-PQ Model	
	Construct	LU-Decomp	Total	#Iters	Total Exec Time (sec)
Sys1	1.06	0.069	1.129	1, 3, 5; 26r	2.92
Sys2	0.571	0.343	0.914	1, 8; 30r	1.13
Sys3	0.063	0.169	0.232	1, 3; 13r	0.264
Sys4	~0	~0	~0	1, 2; 11r	0.0116
Sys5	NA	NA	NA	5r	0.056
Sys6	NA	NA	NA	5r	0.0024

The power flow algorithm has been run for the test systems on a computer with 2.66-GHz Intel Core2 Duo processor. The convergence criteria of 0.05% and 0.02% are used for the root-node current change in radial power flow and the cotree voltage difference in network power flow, respectively. The cpu times are presented in Table II.

Sys1 is a very large distribution system, which is also heavily loaded running at one of its summer-peak periods. For this system, three load steps at $\{0.1\%,\ 5\%,\ 100\%\}$ are used. For the others, two load steps $\{0.1\%,\ 100\%\}$ are applied.

The total execution time for each power flow run, along with the number of iterations, is provided in Table II. For the two radial systems, *Sys5* and *Sys6*, the iterations given correspond to the number of forward/reverse traces (i.e., radial iterations) in which the radial power flow converges ("r" denotes a radial iteration). With looped systems, the number of iterations corresponds to network iterations at each load step. The total number of radial iterations during all network iterations is also given. For instance, the power flow converged on *Sys1* after taking 1, 3 and 5 network iterations at 0.1%, 5% and 100% load steps, respectively, and a total of 26 radial iterations have been performed for the entire simulation. Execution time for sensitivity matrix processing, which may take up a significant portion of network power flow execution, is also presented. The total execution time involves both sensitivity matrix processing and network iterations. Sensitivity matrix processing is represented as the combination of matrix construction and LU-decomposition.

The power flow has also been run on the test network systems to make a comparison of performance with and without the load-stepping approach. As shown in Table III, the systems have been tested for two additional loading levels as they are overloaded by 30% and 60%. The approximate execution times and the number of iterations required for each case are presented in the table.

From Table III it may be seen that for lightly meshed and lightly loaded systems the load stepping process may increase the execution time. However, as systems become more meshed and loaded, the load stepping technique becomes competitively efficient and more reliable when compared to the traditional method. In fact, there may be instances where the load stepping technique can provide faster solution than the traditional approach. Additionally, although not presented in the table, load stepping improves the convergence as systems become very

TABLE III
POWER FLOW PERFORMANCE AS RUN ON TEST SYSTEMS FOR THREE SYSTEM-LOADING LEVELS WITH AND WITHOUT LOAD-STEPPING TECHNIQUE

System	Load Stepping	Exec Time / #Iters		
		100% Load	130% Load	160% Load
Sys1	100%	2.16 sec	2.36 sec	2.43 sec
		5; 15r	6; 21r	7; 24r
	0.1%, 5%, 100%	2.92 sec	3.08 sec	3.29 sec
		1, 3, 5; 26r	1, 3, 5; 29r	1, 3, 6; 32r
Sys2	100%	1.16 sec	1.41 sec	X
		9; 39r	18; 78r	X
	0.1%, 100%	1.13 sec	1.26 sec	1.57 sec
		1, 8; 30r	1, 14; 47r	1, 29; 82r
Sys3	100%	0.271 sec	0.279 sec	0.281 sec
		5; 17r	6; 20r	6; 22r
	0.1%, 100%	0.264 sec	0.275 sec	0.277 sec
		1, 3; 13r	1, 5; 17r	1, 5; 18r
Sys4	100%	0.0073 sec	0.0073 sec	0.0076 sec
		2; 11r	2; 11r	2; 12r
	0.1%, 100%	0.0116 sec	0.0124 sec	0.0280 sec
		1, 2; 11r	1, 2; 12r	1, 5; 18r

heavily loaded. For example, it is observed that when a double contingency (loss of two 33-kV feeders) occurs in *Sys1* at 100% loading, the load-stepping method continues to converge, while the conventional method fails.

For radial systems the factors that affect the convergence properties (number of iterations and execution time) the most are: 1) the total number of components; and 2) the loading level. For meshed systems the number of loops becomes increasingly significant. For very heavily meshed systems, the processing of a large sensitivity matrix consumes most of the execution time.

VI. CONCLUSIONS

This paper has presented several improvements over the forward-backward sweeps method commonly used for the solution of radial and lightly meshed distribution systems. For example, a load-stepping technique that is not very sensitive to the location of the break-points allows for the solution of very heavily loaded systems. As conceived and implemented, the load-stepping technique does not increase the computation effort for heavily meshed systems where, in fact, the execution time could be shorter than with the traditional approach. Another improvement is that the new method is capable of solving systems involving several looped transformers. The approach of this paper does not need to pre-set the voltages of the break points close to their nominal values. The algorithm has been efficiently implemented with the use of modern programming techniques based on iterators. Examples on theoretical and real systems have been presented.

ACKNOWLEDGMENT

The authors would like to thank Consolidated Edison, Detroit Edison, and Ameren for providing circuit models used in this study.

REFERENCES

[1] B. Stott and O. Alsaç, "Fast decoupled load flow," *IEEE Trans. Power App. Syst.*, vol. PAS-93, pp. 859–869, May/Jun. 1974.
[2] W. F. Tinney and C. E. Hart, "Power flow solution by Newton's method," *IEEE Trans. Power App. Syst.*, vol. PAS-86, pp. 1449–1460, Nov. 1967.
[3] P. A. N. Garcia, J. L. R. Pereira, S. Carneiro, Jr, V. M. da Costa, and N. Martins, "Three-phase power flow calculations using the current injection method," *IEEE Trans. Power Syst.*, vol. 15, no. 2, pp. 508–514, May 2000.
[4] L. R. Araujo, D. R. R. Penido, S. Carneiro, Jr, J. L. R. Pereira, and P. A. N. Garcia, "A comparative study on the performance of TCIM full Newton versus backward-forward power flow methods for large distribution systems," in *Proc. IEEE PSCE*, Atlanta, GA, Nov. 2006, pp. 522–526.
[5] W. H. Kersting and D. L. Mendive, "An application of ladder network theory to the solution of three-phase radial load-flow problems," in *Proc. IEEE Power Eng. Soc. Winter Meeting*, New York, Jan. 1976.
[6] D. Shirmohammadi, H. W. Hong, A. Semlyen, and G. X. Luo, "A compensation-based power flow method for weakly meshed distribution and transmission networks," *IEEE Trans. Power Syst.*, vol. 3, no. 2, pp. 753–762, May 1988.
[7] C. S. Cheng and D. Shirmohammadi, "A three-phase power flow method for real-time distribution system analysis," *IEEE Trans. Power Syst.*, vol. 10, no. 2, pp. 671–679, May 1995.
[8] G. X. Luo and A. Semlyen, "Efficient load flow for large weakly meshed networks," *IEEE Trans. Power Syst.*, vol. 5, no. 4, pp. 1309–1316, Nov. 1990.
[9] F. Li and R. Broadwater, "Software framework concepts for power distribution system analysis," *IEEE Trans. Power Syst.*, vol. 19, no. 2, pp. 948–956, May 2004.
[10] D. Zhu, R. P. Broadwater, K. Tam, R. Seguin, and H. Asgeirsson, "Impact of DG placement on reliability and efficiency with time-varying loads," *IEEE Trans. Power Syst.*, vol. 21, no. 1, pp. 419–427, Feb. 2006.
[11] R. P. Broadwater, J. C. Thompson, and T. E. McDermott, "Pointers and linked lists in electric power distribution circuit analysis," in *Proc. 1991 IEEE PICA Conf.*, May 1991, pp. 16–21.
[12] L. R. Feinauer, K. J. Russell, and R. P. Broadwater, "Graph trace analysis and generic algorithms for interdependent reconfigurable system design and control," *Naval Eng. J.*, vol. 120, no. 1, pp. 29–40, 2008.
[13] W. A. Blackwell, *Mathematical Modeling of Physical Networks*. New York: MacMillan, 1968.
[14] M. H. Austern, *Generic Programming and the STL: Using and Extending the* C + + *Standard Template Library*. Reading, MA: Addison-Wesley Professional, 1999.

Murat Dilek received the M.S. and Ph.D. degrees in electrical engineering from Virginia Tech, Blacksburg, in 1996 and 2001, respectively.

He is a Senior Development Engineer at Electrical Distribution Design, Inc. His work involves computer-aided design and analysis of electrical power systems.

Francisco de León (S'86–M'92–SM'02) received the Ph.D. degree from the University of Toronto, Toronto, ON, Canada, in 1992.

He has held several academic positions in Mexico and has worked for the Canadian electric industry. Currently, he is an Associate Professor at Polytechnic Institute of NYU, New York. His research interests include the analysis of power phenomena under nonsinusoidal conditions, the transient and steady-state analyses of power systems, the thermal rating of cables, and the calculation of electromagnetic fields applied to machine design and modeling.

Robert P. Broadwater (S'68–M'71) is a Professor in power systems and software engineering at Virginia Tech, Blacksburg. He works in the area of computer-aided engineering and generic analysis.

Serena Lee (S'85–M'86) received the B.E. degree from SUNY Stony Brook in 1990 and the M.S. degree in electrical engineering from Polytechnic University, New York, in 1996.

She is a Project Manager in the Research and Development Department at Consolidated Edison Co. of New York, Inc. Her work involves power distribution systems design, operation, and maintenance.